

# N75 27193

## GROUND EFFECTS ON LORAN-C SIGNALS

D. C. Pearce and J. W. Walker  
Communications/Automatic Data Processing Laboratory  
U. S. Army Electronics Command

### ABSTRACT

In conjunction with the test and evaluation of the position fixing capabilities of the Army Manpack Loran Receiver AN/PSN-6, an extensive series of time difference and signal amplitude measurements were made within a 100 km map grid square encompassing Fort Monmouth, New Jersey. The test location is within the coverage area of the East Coast Loran-C Chain. The data were used to develop a simple "smooth-earth" model for the test area as well as to estimate the magnitude and distributions of deviations from this model. Local propagation processes associated with topographic features and the grid of overhead wires in the test area are shown to contribute to the deviations from the model.

### INTRODUCTION

As part of a broad program to develop a capability for navigation and position fixing, the Army is in the process of developing a manpack loran receiver. The position fixing function of the receiver is to provide a real time display of either the loran time difference coordinates or the geodetic coordinates of the receiver position. This conversion between the time difference and geodetic coordinate systems is accomplished by a small computer within the receiver. The research described here was designed to provide a data base for development of simple conversion algorithms as well as to provide an error budget for the resulting conversion. Since a fundamental variable of a loran system is the propagation time of the 100 kHz signal and since the manpack loran receiver is designed to operate on the ground, the present research was planned to provide information on ground wave propagation at the surface of the earth. These propagation results are the subject of this paper.

## BACKGROUND

The fundamental equation describing the functional relationship between a loran time difference and the loran chain parameters is

$$TD(P) = [(D_s - D_m)/C] + ED, \quad (1)$$

where TD(P) is the loran time difference at a field point P,  $D_s$  is the great circle distance from the slave transmitter to the point P,  $D_m$  is the great circle distance from the master transmitter to the point P, C is the propagation velocity of the loran signal, and ED is the emission delay, that is the sum of the propagation time from the master to the slave transmitter and the coding delay introduced at the slave station. [See Footnote (a).]

The non-constant propagation velocity, which varies with the density and amplitude of terrain features and the electrical properties of the overland path, severely limits the utility of Eq. (1) for time difference estimation. On the other hand, the ground wave propagation velocity over sea water is a well-known quantity, so Eq. (1) is very useful for this application. A complete knowledge of the propagation velocity for all propagation paths is necessary for rigorous use of Eq. (1). This procedure requires an extremely large volume of data and clearly is not practical for a manpack loran receiver. This fact furnished the impetus for the development of simplified coordinate conversion algorithms. In essence, the approach was to develop a simple local conversion model based on calibration and to investigate the accuracy characteristics of that model. The reader is referred to the work of Johler [1] and to the references cited therein for details on the complete treatment of overland loran propagation.

## EXPERIMENTAL PROCEDURE

The test area in New Jersey is the 100 km square, 18T WV of the Universal Transverse Mercator Map System. A specially equipped four-wheel drive mobile unit was used during data acquisition. Present instrumentation includes 2 military loran receivers, a timing receiver system with rubidium standard, and ancillary items including printers, oscilloscopes, and power supplies. The military receivers used roof-mounted whip antennas whereas the timing receiver used a rotatable roof-mounted loop antenna.

The calibration procedure is relatively simple, namely to obtain time difference readings at sites of known geodetic control. To obtain estimates of loran receiver performance, approximately 100 time difference measurements were made with each receiver at each site. These measured values were then averaged to provide a time difference for each site. To eliminate separate site surveys, easily identifiable topographic locations, such as road intersections, were used for geodetic control. Coordinates of all sites were determined from 7.5 minute USGS topographic maps. Criteria for site selection were positive identification, freedom from strong electromagnetic scatterers, and accessibility with the mobile unit. In general, the absence of power lines was the most difficult criterion to meet. Several of the sites were at geodetic bench marks which provided a higher order geodetic control.

The distribution of calibration sites is shown in Fig. 1. The numbers shown in this figure are primarily for site identification purposes, but are also related to the time of calibration. Data at sites identified with numbers less than 1000 were obtained in December 1972, whereas those with identifiers greater than 1000 were obtained in July 1973. This latter study was designed to give an increased calibration density within a 60 km square located in the SE corner of the primary test area. In addition, the absence of nearby power lines was of extreme importance. It is estimated that for these locations, there were no wires within one kilometer of the site. For the December 1972 measurements there were no wires within 300 meters of a site. This consideration of the proximity of overhead wires led to the classification of first and second order TD data, as indicated in Fig. 1.

In October 1973, the timing receiver was used to obtain field strength information at the sites with identifiers less than 1000. Time difference measurements were also obtained to check the repeatability of earlier measurements.

A study of the absolute phase variations of the Loran-C transmissions was initiated in October 1974. The sites for a ray path to the SS7-Y, Nantucket transmitter are designated as phase track points in Fig. 1. All measurements were made relative to the reference point 1480 in Fig. 1. This point is approximately 1 km from the coast. The other sites are at approximately 10 km intervals along the ray path. The experimental procedure was to initialize at the reference point, make phase measurements at other sites, and then close the traverse at the reference site. Each

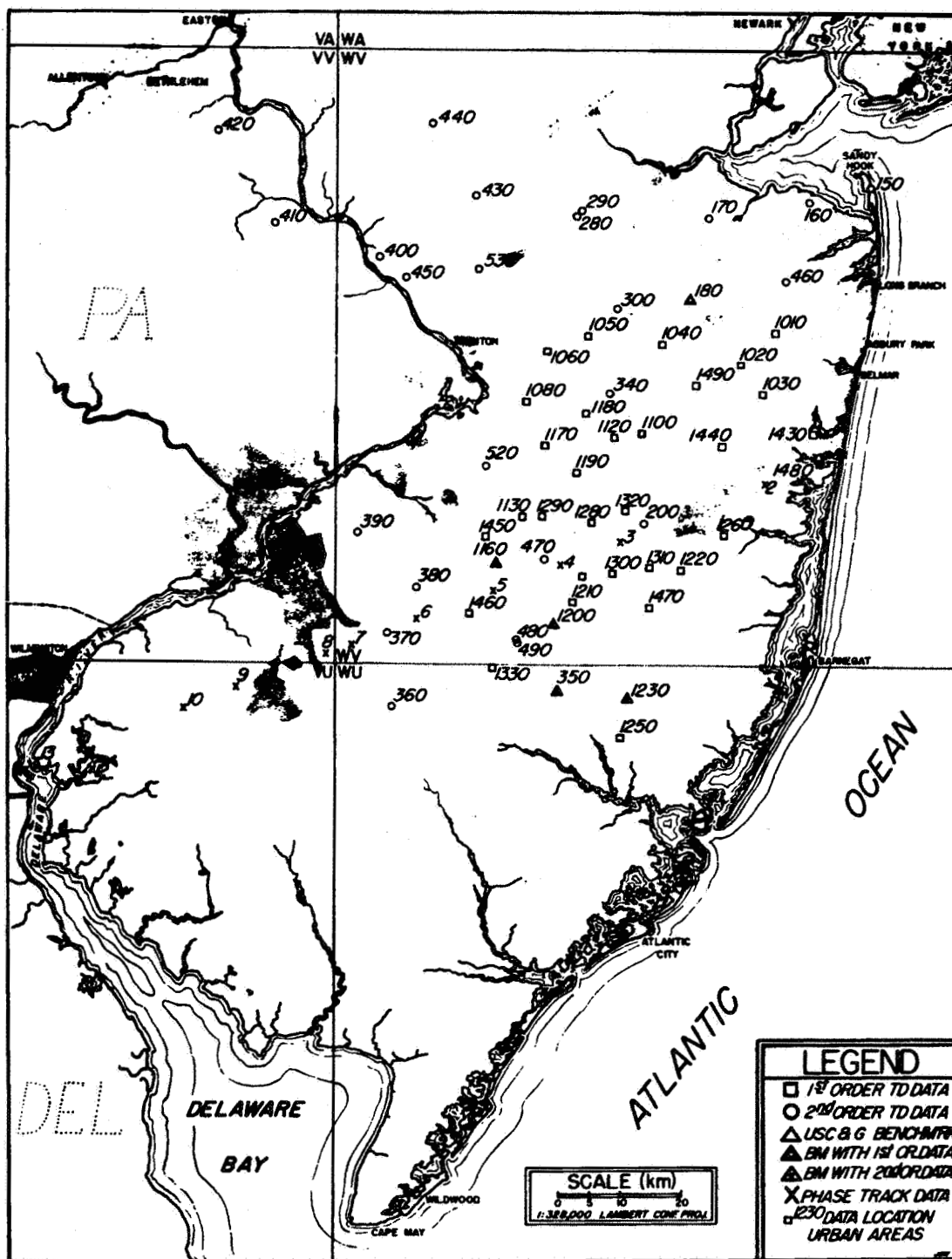


Fig. 1. Map of New Jersey Showing Locations of Loran-C Time Difference and Phase Data Measurements.

series of measurements required from 6 to 8 hours. Closing the traverse at the reference site provided an estimate of the frequency offset of the rubidium standard.

The test area is a segment of the coastal plain which is essentially devoid of pronounced terrain features and conductivity discontinuities. Thus no significant perturbations of the loran signals were expected from these sources.

#### ANALYTICAL PROCEDURE

The model adopted for data analysis is a modification of Eq. (1). The underlying assumption for this model is that for modest coverage areas, a constant overland propagation velocity will provide a useful approximation. The equation is:

$$TD(P) = (ED + \alpha) + \beta(D_s - D_m) + \epsilon(\theta_s, \theta_m). \quad (2)$$

In this expression,  $\alpha$  and  $\beta$  are arbitrary parameters to be determined by least squares analysis of the measured data. The correction function,  $\epsilon(\theta_s, \theta_m)$ , is to account for sea water paths at a bearing angle  $\theta$  from the slave and master transmitters to the field point. This function is included to account for the significant difference between ground wave propagation velocity over land and over sea water. The parameter  $\alpha$  can be interpreted as an average time difference offset characteristic of the test area. The parameter  $\beta$  can be interpreted as the reciprocal of the local propagation velocity. However, in view of the simplicity of the model and the statistical method of analysis, strict physical interpretation of these parameters should be approached with caution. [See Footnote (b).]

For data processing, the variables  $D_s$  and  $D_m$  were calculated using the method of Sodano and Robinson [2] for the Clarke 1866 spheroid [3].

The correction  $\epsilon(\theta_s, \theta_m)$  was constructed from tabulated functions of the sea water path length as a function of bearing angle from the Nantucket and Carolina Beach transmitters. The sea water path functions were prepared from maps in increments of  $5^\circ$  in the bearing angle. The path length for intermediate bearing angles was determined by linear interpolation. The sea water path length functions are shown in Figs. 2 and 3 for the Carolina Beach and

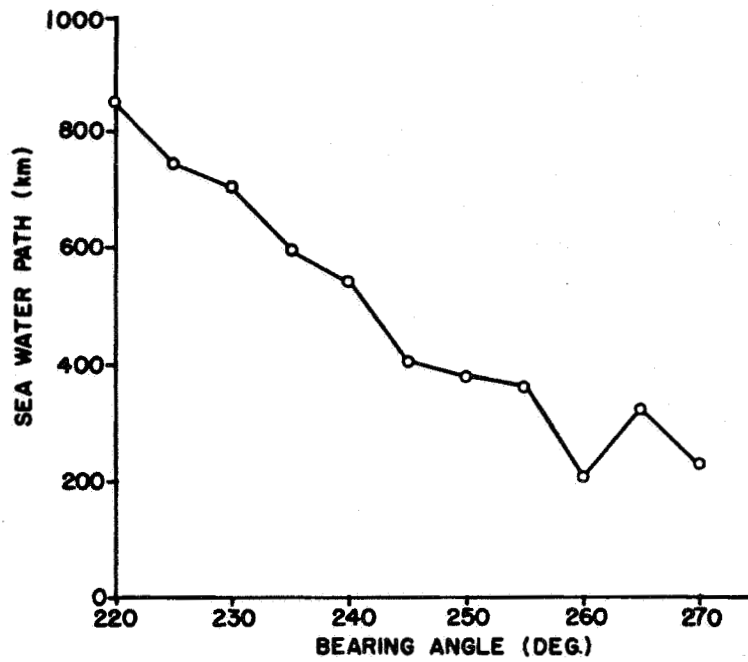


Fig. 2. SS7-Y (Nantucket) Sea Water Path vs. Bearing Angle.

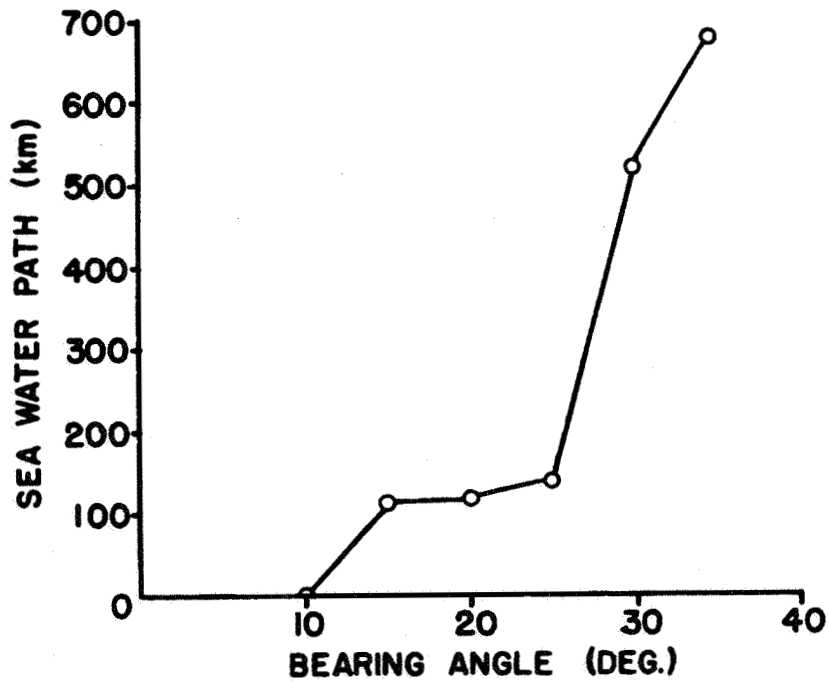


Fig. 3. Master (Carolina Beach) Sea Water Path vs. Bearing Angle.

Nantucket transmissions. In view of the simple interpolation procedure, the error associated with path length determination will be greatest for bearing angles greater than 25° for the Carolina Beach transmission. For this reason, all points with Carolina Beach bearing angles greater than 25° were not considered in the data analysis. This selection process left 61 calibration sites within the 100 km square.

The correction function is

$$\epsilon(\theta_s, \theta_m) = k[L_s(\theta_s) - L_m(\theta_m)] \quad (3)$$

In this expression,  $L_s(\theta_s)$  is the sea water path length at a bearing angle  $\theta_s$  from the slave transmitter and  $L_m(\theta_m)$  is the sea water path length at a bearing angle  $\theta_m$  from the master transmitter,  $k = [(1/C_l) - (1/C_s)]$  where  $C_l$  is the ground wave propagation velocity over land and  $C_s$  is the ground wave propagation velocity over sea water. The values used for these constants are:  $(1/C_l) = 3.3416 \mu\text{s}/\text{km}$  and  $(1/C_s) = 3.3384 \mu\text{s}/\text{km}$ . Thus the constant  $k$  has the value  $0.0032 \mu\text{s}/\text{km}$ . The value of  $C_s$  was obtained from the tables of Johler and Berry [4]. The value of  $C_l$  was estimated from calibration of a geologically similar area in North Carolina where no sea water correction was required.

#### ANALYTICAL RESULTS

As discussed previously, the data processing was designed to give the parameters  $\alpha$  and  $\beta$  for the Nantucket and Dana slave configurations by the method of least squares. To evaluate the effect of coverage area size, the data were treated in two sets. One set included the total of 61 points. The second set included the points within a 60 km square in the SE corner of the 100 km square.

The analytical results are shown in Tables I and II. Also shown are the RMS deviations of the least squares fit for each data set.

TABLE I. STATISTICAL PARAMETERS FOR 100 km SQUARE  
(61 Data Points)

Transmission Pair	$\alpha$ ( $\mu\text{s}$ )	$\beta$ ( $\mu\text{s}/\text{km}$ )	RMS Deviation for Set
SS7-Y	0.85	3.346	0.33
SS7-Z	-0.19	3.339	0.33

TABLE II. STATISTICAL PARAMETERS FOR 60 km SQUARE  
(30 Data Points)

Transmission Pair	$\alpha$ ( $\mu\text{s}$ )	$\beta$ ( $\mu\text{s}/\text{km}$ )	RMS Deviation for Set
SS7-Y	0.74	3.346	0.22
SS7-Z	-4.11	3.349	0.25

An estimate of the experimental uncertainties was obtained by statistical analysis of the data acquired at each site. This procedure yielded an average value of  $0.15 \mu\text{s}$  attributable to instrumental jitter. In addition, it has been estimated that the use of topographic maps introduces a location uncertainty of the order of 20 meters. For the test area, this corresponds to a time difference error of about  $0.1 \mu\text{s}$ . Therefore, experimental processes are estimated to contribute an uncertainty of the order of  $0.18 \mu\text{s}$ .

The distribution of the magnitude of the time difference deviations is shown in Figs. 4 and 5 for the Nantucket-Carolina Beach (SS7-Y) and the Dana-Carolina Beach (SS7-Z) configurations, respectively. The solid curves are the normal distributions corresponding to the standard deviations calculated for each slave configuration. The areal distribution of the time difference deviations for each slave configuration is shown in Figs. 6 and 7.

The results of the field strength study of October 1973 are shown in the contour plots of Figs. 8 and 9 for the Nantucket and Dana transmissions, respectively. The contour



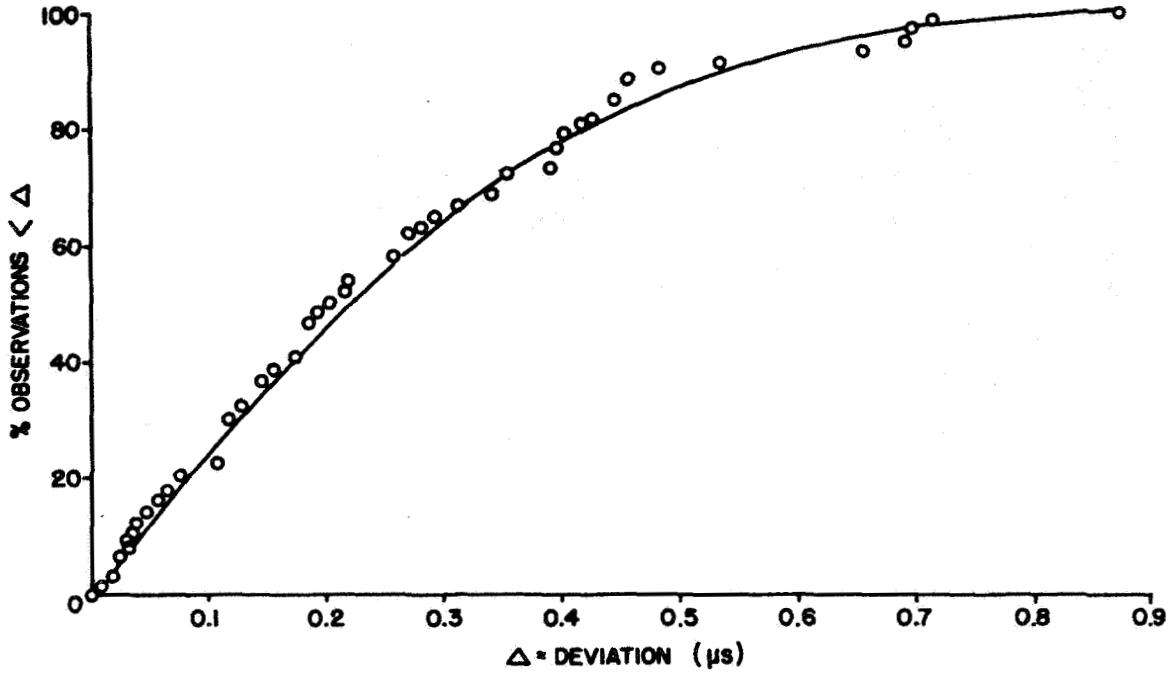


Fig. 4. SS7-Y Time Difference Deviation Magnitude Distribution.

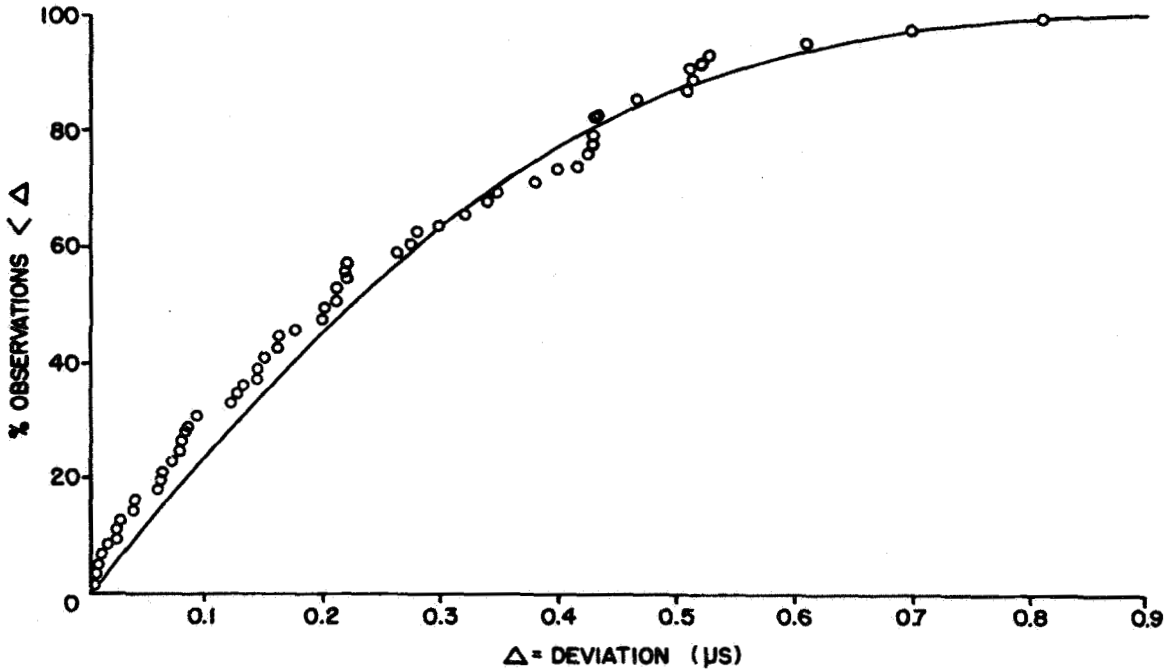


Fig. 5. SS7-Z Time Difference Deviation Magnitude Distribution.

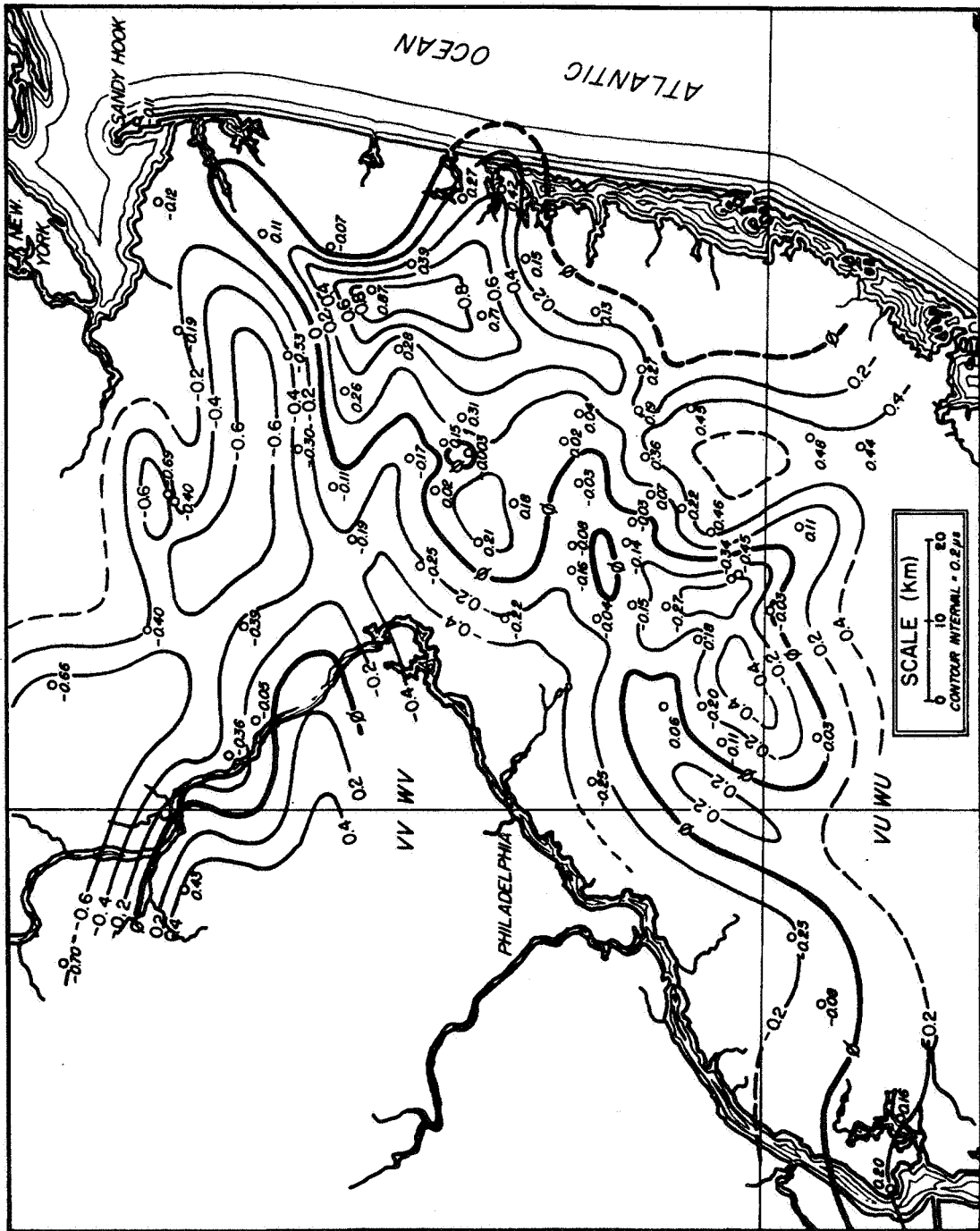


Fig. 6. Map Showing SS7-Y Time Difference Deviations from Theoretical Model.

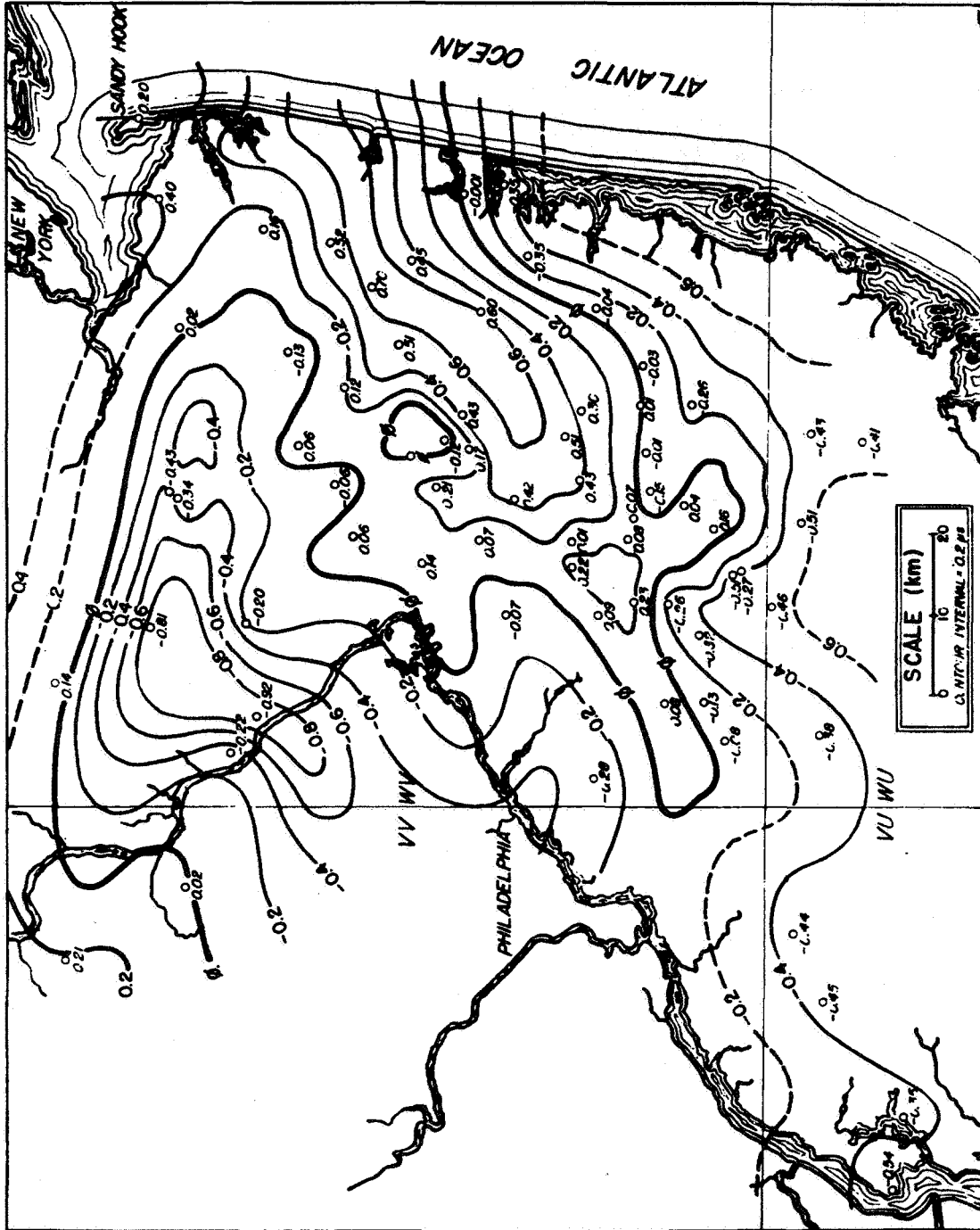


Fig. 7. Map Showing SS7-Z Time Difference Deviations from Theoretical Model.

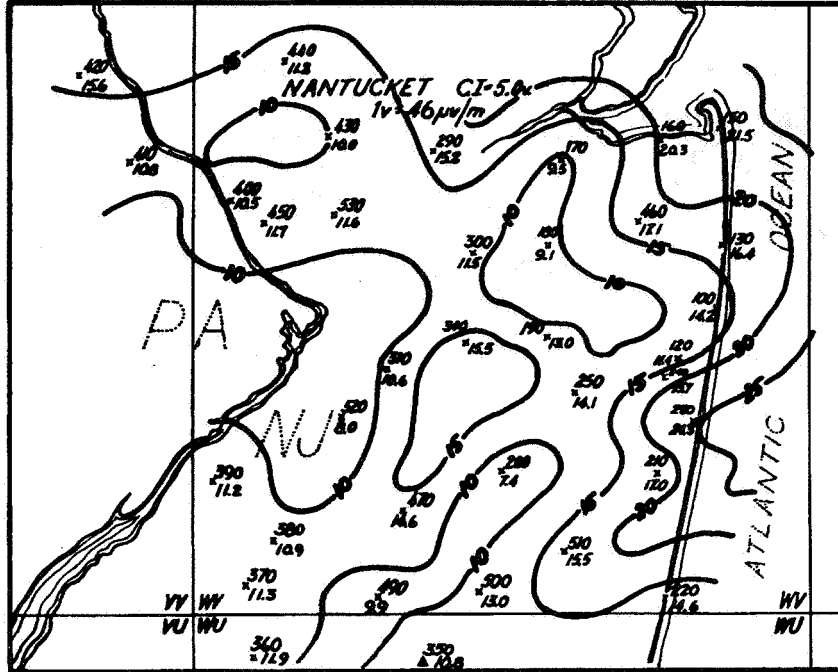


Fig. 8. Map Showing SS7-Y Field Strength Distribution.

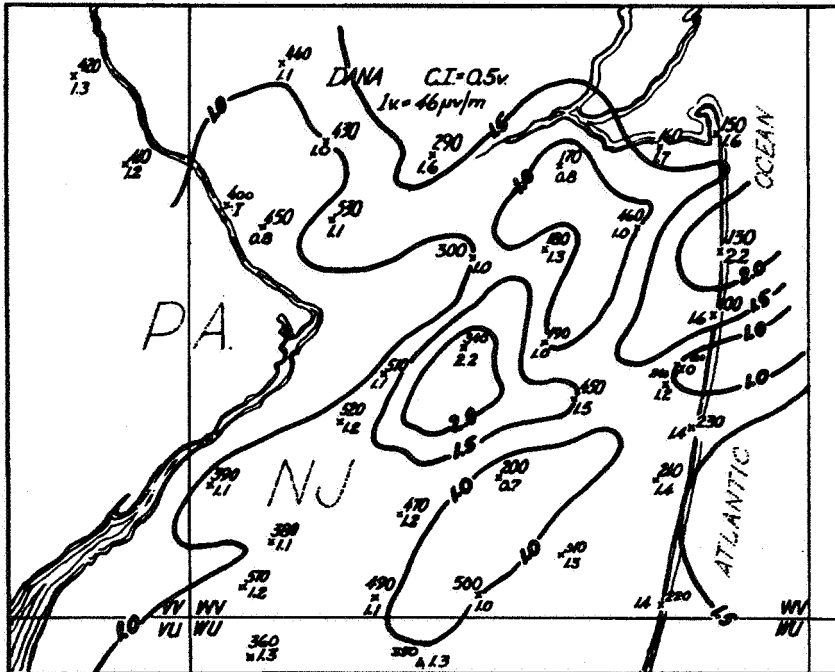


Fig. 9. Map Showing SS7-Z Field Strength Distribution.

values are the output voltage of the amplitude strobe of the timing receiver when tracking the third cycle crossover with an input attenuation of 40 dB. The indicated conversion constant of 46  $\mu\text{v}/\text{m}/\text{volt}$  was estimated from the antenna characteristics to provide a corresponding approximate value of the field strength.

The phase of the Nantucket transmission relative to the reference point as a function of the distance from the transmitter is shown in Fig. 10. The plotted points are an average of measurements on six different days. The deviations of these measurements from a least squares fitted straight line are shown in Fig. 11. The experimental results have been corrected for loran chain variations from data furnished by the United States Coast Guard. The error bars in Fig. 11 represent typical uncertainty estimates arising from rubidium standard frequency offset.

#### DISCUSSION AND CONCLUSIONS

The simplified mathematical model presented provides a reasonably accurate description for a small segment of the coverage area, namely the 100 km square area. The observed magnitude of the deviations from the model are randomly distributed. Specific parameters of the model are sensitive to the size of the coverage area. In view of the simplicity of the model, strict interpretation of the parameters in terms of propagation properties is not possible. For example, the value of the parameter  $\beta$  for the SS7-Z slave shown in Table I (3.339  $\mu\text{s}/\text{km}$ ) is essentially the value expected for an all sea water path. [See Footnote (c).]

The time difference deviations and field strengths exhibit a pronounced areal variation. Furthermore, the contours of both variables exhibit a preferred orientation in a NE-SW direction. Figure 12 shows salient topographic and geological features of the test area. These features also exhibit a preferred orientation in a NE-SW direction. Consequently, there appears to be some correlation between contour orientation and the topographic and geological features.

The standard deviations of the time difference data are 0.33 and 0.22  $\mu\text{s}$  for the 100 km square and the 60 km square, respectively. These values exceed the 0.18  $\mu\text{s}$  estimated to arise from experimental sources. Clearly the results for the smaller test area are in better agreement with the theoretical model than are the results for the larger test area. The criterion for proximity of nearby overhead wires

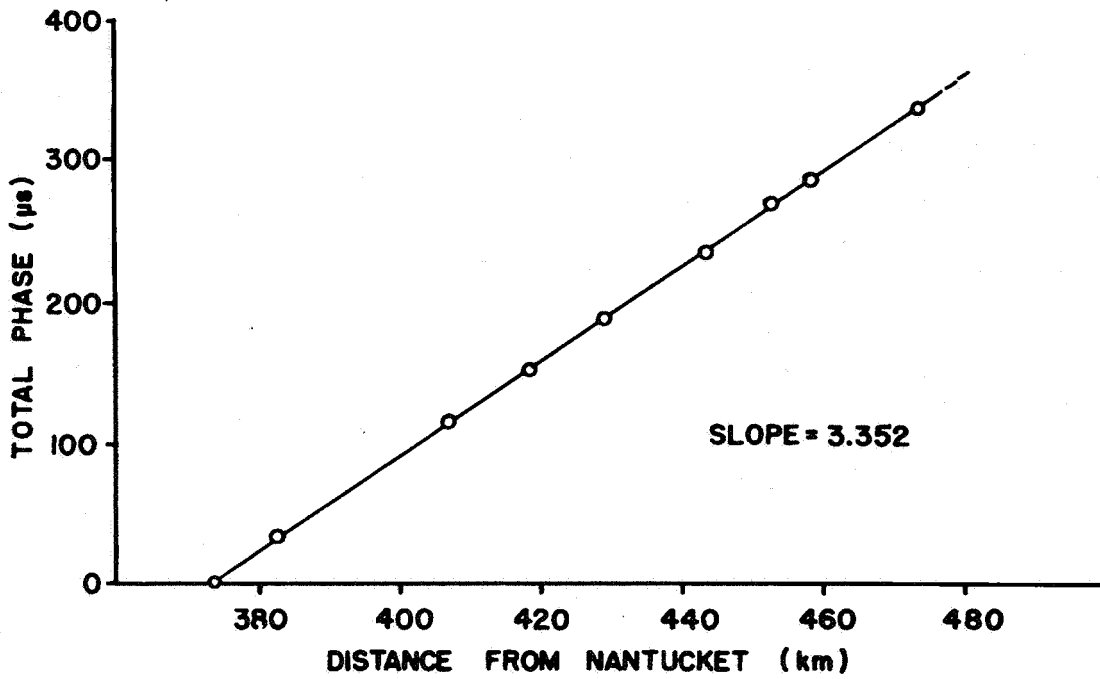


Fig. 10. SS7-Y Phase Variation vs. Distance.

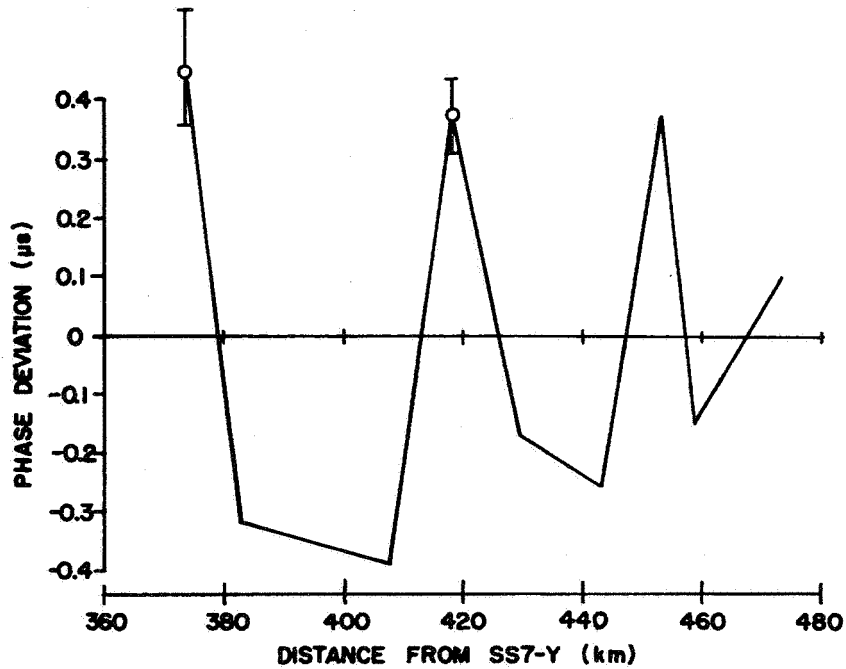


Fig. 11. SS7-Y Phase Deviation vs. Distance.

also influences the deviations from the theoretical model. Although the time difference data does not allow a definitive separation of the contributions of area size and proximity of overhead wires, both factors, as well as previously discussed topographic effects, appear to contribute to the deviations from the idealized model.

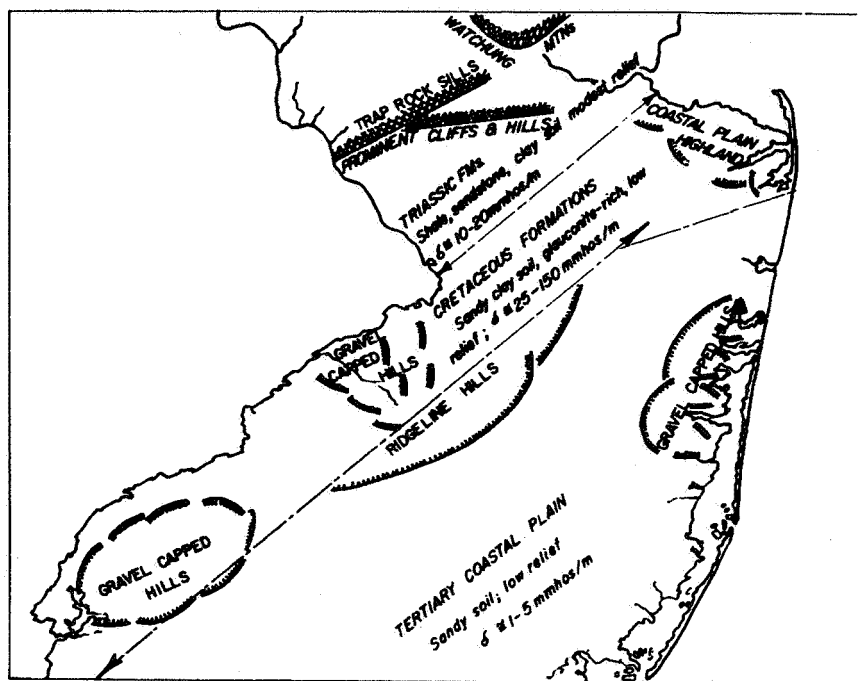


Fig. 12. Map of New Jersey Showing Salient Topographic and Geologic Features.

Preliminary measurements of absolute phase along a ray path from the Nantucket transmitter across the 100 km test area, yielded a linear variation of phase with distance from the transmitter. The least squares slope is  $3.352 \mu\text{s}/\text{km}$ , with a standard deviation of  $0.3 \mu\text{s}$ . These observations are considered to be consistent with the time difference measurements for the 100 km square. Since this particular ray path is located in a region of nearly constant conductivity and is devoid of terrain irregularities, it is assumed that the major contribution to the observed deviations arises from scattering associated with overhead wires.

These results are of importance to the position fixing accuracy of ground-deployed loran receivers. Randomly distributed time difference deviations of the order of 0.3  $\mu$ s from an idealized model have been observed. This study suggests that scattering associated with topographic features as well as from man-made sources such as overhead wires contribute to the deviations. The results yield a realistic standard deviation of position location accuracy of the order of 60 meters.

#### ACKNOWLEDGMENTS

The authors are indebted to Lt(jg) A. A. Sarra, Jr., Coast Guard Loran Station, Carolina Beach, North Carolina, and to LCdr A. R. Trivers, Coast Guard Electronic Engineering Center, Wildwood, N. J., for assistance in obtaining information on the East Coast Loran Chain during October 1974.

The assistance of Mr. H. Garber and Mr. A. H. Zanella, USAECOM, in obtaining the field data is gratefully acknowledged.

A portion of the funding support for this research was provided by the Office of the Project Manager, Navigation and Control Systems (NAVCON), Fort Monmouth, New Jersey.

#### REFERENCES

- [1] Johler, J. R., (1971), Loran radio navigation over irregular inhomogeneous ground with effective ground impedance maps, OT/ITS Research & Engrg. Report 22 (Supt. of Documents, U. S. Government Printing Office, Washington, D. C. 20402).
- [2] Sodano, E. M. and T. A. Robinson, (1963), Direct and inverse solutions of geodesics, Army Map Service, Technical Report No. 7 (Rev.).
- [3] Department of the Army (1967), Grids and Grid References, Department of the Army Technical Bulletin TM 5-241-1.
- [4] Johler, J. R., and L. A. Berry, (1967), Loran-D phase corrections over inhomogeneous irregular terrain, ESSA Technical Report IER 59-ITSA 56 (Supt. of Documents, U. S. Government Printing Office, Washington, D. C. 20402).



### Additional Background Information

- (a) The assumption of identical propagation velocities over the paths  $D_s$  and  $D_m$  is implicit in Eq. (1).
- (b) The interpretation of  $\beta$  as the reciprocal of a local propagation velocity is valid only to the extent that the propagation velocities over the paths  $D_s$  and  $D_m$  are identical.
- (c) Furthermore, a change in the parameter  $\alpha$  of 4  $\mu$ s for two fits of the same area is devoid of physical significance. This behavior is related to the fact that  $D_s$  and  $D_m$  are large quantities so that in the least squares process, small variations in the parameter  $\beta$  are compensated for, by large variations in the parameter  $\alpha$ . Additional physical constraints as discussed by Doherty [5] are necessary for a realistic physical interpretation of a statistical model.

---

[5] Doherty, R. H., (1972), A Loran-C grid calibration and prediction method, OT/TRER 25 (Supt. of Documents, U. S. Government Printing Office, Washington, D. C. 20402).